Chapter 7

Addressing The Problem

7.1 Introduction

The goal of this thesis is to develop a classifier which discriminates between surfaces on the basis of their visual appearance. The development of such a classifier is described in Chapter 5. However, using the models developed in the earlier chapters it is shown in Chapter 6 that the direction of illumination is a critical factor in the performance of the classifier. This chapter will review a range of candidate techniques on which a classifier that is robust to tilt variations may be based. One technique will be selected for further investigation in the next chapter.

Having observed the effect, we now consider some techniques aimed at reducing tilt induced misclassification error. Chantler proposed four schemes [Chantler94], we will begin by discussing all four and evaluating the three which we believe most appropriate to the terms of this thesis. Since we wish to classify textures on the basis of their surface properties, we then proceed to review the field of shape from shading. Finally, we propose a novel scheme which uses a model based technique to overcome the problem of tilt induced classifier failure.

7.2 Review of Chantler's Feature Space Proposals

In [Chantler94] Chantler proposes four techniques for conferring tilt-robustness on a classifier:

(i) a single classification rule obtained by training over the tilt range,

(ii) a series of rules indexed by tilt,

(iii) a segmentation based technique, and

(iv) a filter based technique designed to reverse the directional effects of illumination.

The first three techniques operate in feature space, whereas the last pre-processes the image before feature extraction. In his thesis, Chantler chose to investigate only the last option. In this work we will discuss each and investigate those which are relevant to this thesis.

7.2.1 Multiple Training Samples

Chantler’s first proposal is to train the classifier over the range of illuminant conditions it is likely to encounter. He notes that the increased variance of each class may reduce classification accuracy and pursues the idea no further. We reconsider the scheme in the following terms:

In Chapter 5 we introduced a discriminant which classified a pixel, with feature vector ***F***, as having label $\hat{l}$ on the criterion shown below:

$$\hat{l}(\mathbf{F}) = \underset{l_i}{\arg\max}\,[(p_{\mathbf{F}|l_i}(\mathbf{F}|l_i))\ ]$$

where $p_{\mathbf{F}|l_i}(\mathbf{F}|l_i)$ is the probability density function of feature ***F***, given that a pixel belongs to class *i*.

In Chapter 6 we showed that the probability density function of vector ***F***, $p(\mathbf{F}|l_i)$, is a function of the illuminant tilt. We treat tilt angle as a random variable, randomly distributed between 0 and 2π, and describe using the joint pdf:

$$p(\mathbf{F}, \tau\ |l_i)$$

Chantler's proposal attempts to classify pixels on the basis of an approximation to the marginal density of *p*. The marginal distribution will be the integral of the joint density over tilt (7.2.1a), assuming the illuminant tilt angle is drawn from a uniform distribution, and the feature distributions vary continuously. This can be approximated by the summation of a finite number of sample distributions (7.2.1b).

$$K(\mathbf{F}\ |l_i) = \int_0^{\pi} p(\mathbf{F}, \tau\ |l_i)\,d\tau \qquad (7.2.1a)$$

$$K'(p) = \sum_{\tau=0}^{\pi} f(\mathbf{F}, \tau \mid l_i) \tag{7.2.1b}$$

Where classification is made on the basis of:

$$\hat{l}(\mathbf{F}) = \underset{l_i}{\arg\max} \left[(K_{\mathbf{F}|C_i}(\mathbf{F}|l_i)) \right]$$

The probability function $K_i(p)$ will occupy at least an equal, or more probably, a larger volume of feature space than any of its component (tilt conditional) density functions. There will consequently be a greater degree of overlap between clusters of different classes. The success of the classifier is dependent on the degree of tilt induced cluster movement being small relative to the distribution separation. In *Figure 7.2.1* we plot the feature means derived from filters oriented at 0° and 90° which have been applied to the exemplar textures: *Rock* and *Striate*.

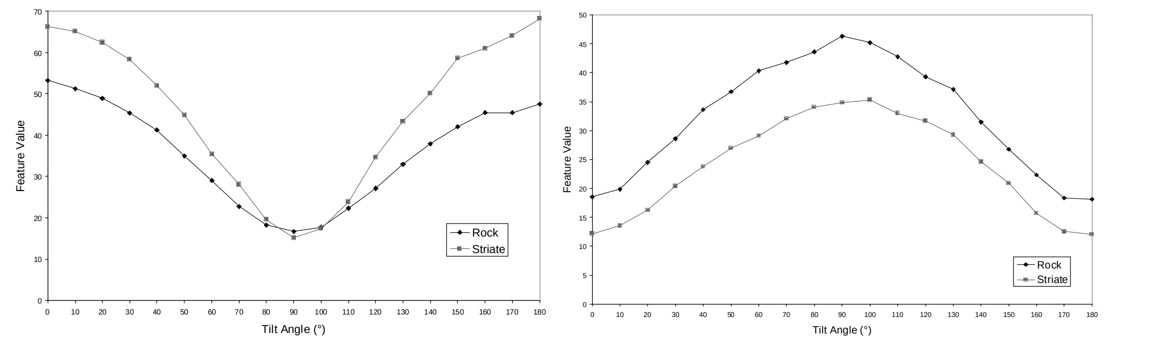

Figure 7.2.1 Feature means for Rock and Striate textures calulated from F25 filters oriented at 0° and 90°.

In *Figure 7.2.1*, it is shown that the assumption that cluster separation is large relative to cluster movement is not reasonable for the texture features measured on the *Rock* and *Striate* textures. While the clusters may or may not overlap at a given tilt, the movement of the means with tilt, in both cases, clearly show that it is not possible to set a single threshold to discriminate between the textures throughout the tilt range.

Although this technique is not appropriate in the above case, we have not ruled out the possibility that it may be effective for data sets which are well separated in feature space. While the technique is not universally applicable to the tilt problem, its simplicity of implementation makes it worthy of investigation for a given data set. We also conclude from the inadequacy of a single threshold that *a priori* knowledge of the illuminant tilt angle is a necessary condition for the illuminant invariant classification of rough surfaces. This leads us to Chantler's second proposal.

7.2.2 Multiple Discriminants

Chantler's second proposal uses multiple training samples captured under various illumination conditions to build a library of discriminant functions which can then be indexed by tilt angle. Any practical system will have a finite number of training samples. In the context of the schemes considered later in this chapter, we limit ourselves to three training images.

We conducted experiments on the *Anaglypta* and both the *Stone* montages, in each case using three discriminants, developed at 0°,90° and 180°, switching between discriminants at 50° and 140° respectively.

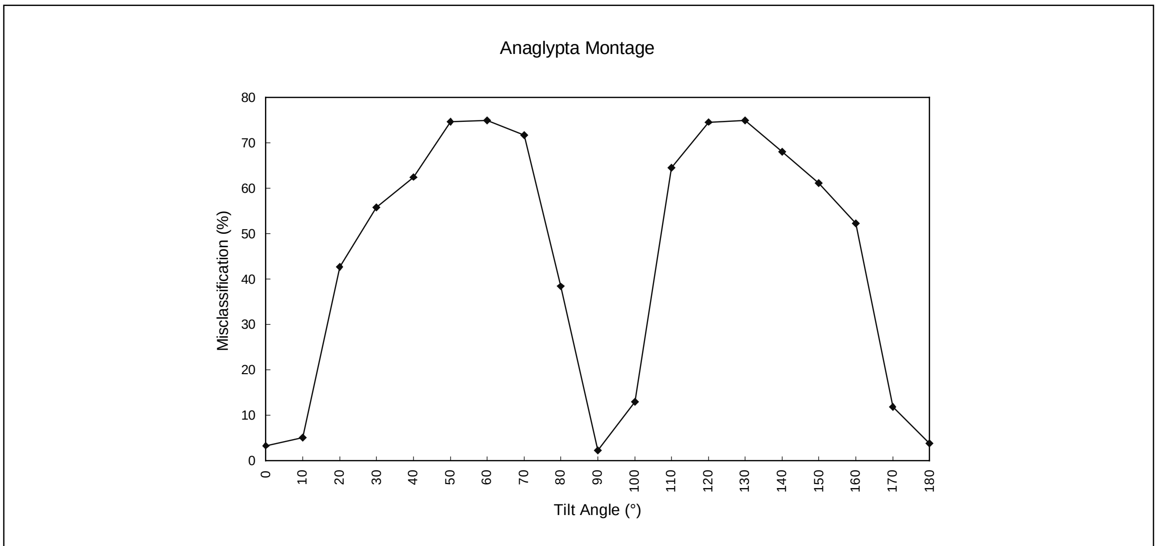

Figure 7.2.2 The use of three discriminants with the anaglypta montage.

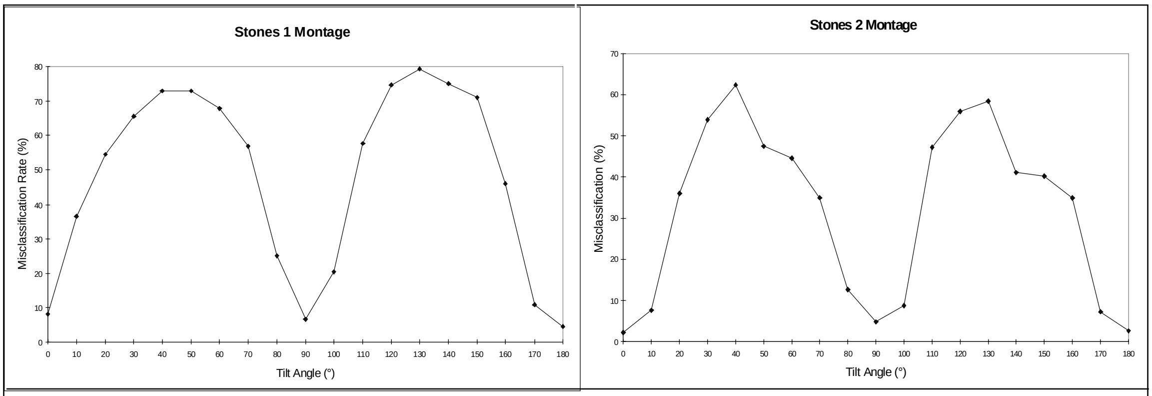

Figure 7.2.3 The use of three discriminants with Stone montages.

As we might expect, the misclassification graph has minima at 0°,90° and 180°. However, the majority of intermediate points show an unacceptably high misclassification rate. The speed with which classification errors increase as we move away from the training angle also suggests that the necessary interval between training samples is so small, certainly less than 20°, as to be uneconomical for a practical classification system. This immediately suggests an interpolative scheme, however non-linearities in both the imaging and the classification processes make this problematic. Later in this chapter we will propose a technique that is a derivative of this scheme, but which operates in image, rather than feature space, circumventing the problems of non-linearity.

7.2.3 Segmentation/Classification

The rationale for this scheme is that since the problem is caused by movement of clusters across discriminant boundaries an appropriate strategy is to track the clusters using cluster analysis techniques. The postulated clusters then may be identified as belonging to an *a priori* defined class at a higher level in the image understanding hierarchy. Identification at this level would be carried out by some feature measure (Chantler suggests features based on the power spectra) which for reasons of computational cost, or the requirement for homogenous regions of data, could not be effectively integrated into the lower levels. We note that cluster analysis is being used as a segmentation tool, and is therefore interchangeable with other segmentation techniques, such as edge-based or region growing approaches. This scheme is effectively an unsupervised technique, and consequently outwith the terms of this thesis. We do not investigate it further.

7.3 Chantler's Filters

While Chantler proposed four techniques he selected only one for further investigation. Unlike the earlier techniques which seek to deal with the feature space effects of tilt variation, this technique is proactive, and seeks to remove, or at least mitigate the effects of tilt before features are extracted.

7.3.1 Review

Chantler proposed and evaluated a system of filters to reduce the effect of tilt effects on the classification of texture [Chantler94]. After verifying Kube's work on real textures, Chantler used this model as the basis on which he could develop a frequency domain technique to remove the directional effect introduced by illumination—treating the problem essentially as one of inverse filtering. In this section we consider four issues that arise from this scheme.

- *Linearity*: the filters are subject to the restrictions on surface type and lighting conditions considered in Chapter 3. Chantler attempted to model the effects of non-linearity by adding an empirical term, *b*, to form his F1 filter class (7.3.1a). In effect treating the unwanted signal components as additive white noise.

$$H_{F1}(\omega,\theta) = \frac{1}{m\left|Cos(\theta-\tau)\right| + b} \qquad (7.3.1a)$$

where

m and *b* are empirically derived coefficients.

- *Frequency dependency*: if we attempt to fit the F1 model to radial plots taken at different frequencies we find a significant radial frequency dependency in both terms. This led Chantler to develop the modified F2 model, where the second order parameters are estimated in a two stage process: first, radial plots are taken for overlapping frequency ranges, the *m* and *b* parameters are fitted to each using least squares; second a linear least squares model is fitted to each parameter as a function of frequency.

$$H(\omega,\theta) = \frac{1}{m(\omega)\left|Cos(\theta-\tau)\right| + b(\omega)} \qquad (7.3.1b)$$

- *Directionality*: as the estimation process can only be applied to isotropic or near isotropic textures, it assumes that directional textures, for which parameters cannot be estimated, will be similarly affected by changes in tilt. In Chapter 3 it was shown that rough directional surfaces do exhibit behaviour incompatible with Kube's model. In combination with the linearity restrictions this forms a significant limit to the utility of the scheme. The degree of restriction is illustrated by the fact that the isotropy condition, strictly applied, would rule out all the test montages.

• *Optimality*: The work reported in Chapter 3 was based on the performance of a filter which was optimal for a particular texture. In a classification problem, we must accept the fact that any general filter will be sub-optimal for each texture. If we reconsider the frequency variation of model parameters with frequency for different textures we see that there is a wide variation from texture to texture. Chantler tackled this problem by averaging the model parameters for each texture. Whether the resulting sub-optimal filter will be sufficiently effective will depend on the similarity of the textures. This interdependency limits the generality of any experimental results obtained.

In order to address these issues, prior to an evaluation of the technique, a new set of synthetic textures *Figure 7.3.1* is introduced.

• *Linearity:* in chapter 3 we concluded that the major factor affecting how well a linear model describes rendering is the rms slope of the surface. The rms slopes of the synthetic surfaces are shown in *Table 7.3.1*.

• *Directionality*: the requirement for isotropic surfaces is satisfied by using Malvaney and fractal surface models.

• *Frequency dependency:* The synthetic textures can be used to gauge the effect of frequency dependency in the optimal parameter values. The distinct radial frequency characteristics of the fractal and Mulvaney models provides one point of comparison. The fractal surfaces (1 and 2) differ in their roll-off rates, β=3.0 and 4.5 respectively. The Mulvaney surfaces differ in the cut-off frequency at which the transition between white noise and fractal roll-off occurs.

• *Optimality:* The issue of optimality is accomodated into the evaluation in two steps. Firstly, experiments are carried out on a texture by texture basis. In each case the filter is designed purely for that texture. In the second stage the filter parameters of the texture specific filters are averaged to produce a general filter which is applied to all the textures in the montage.

The spectra and rms slope of the surfaces are shown in *Figure 7.3.2* and respectively.

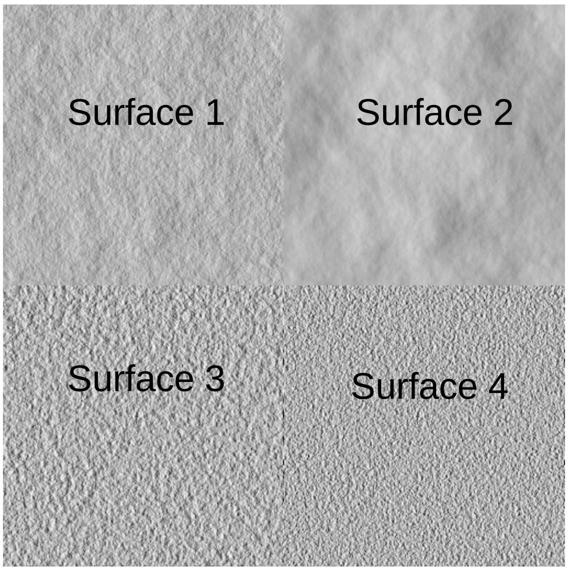

Figure 7.3.1 Isotropic texture montage.

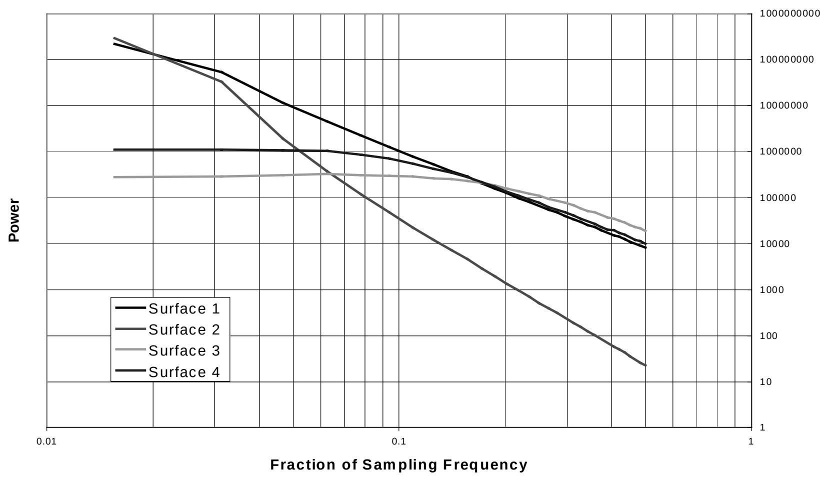

Figure 7.3.2 Spectra of isotropic surfaces.

Surface	m_{rms}
1	0.0924
2	0.0653
3	0.249
4	0.223

Table 7.3.1 RMS Slopes of test surfaces.

7.3.2 A Texture Specific Filter

In the last section it was concluded that a significant limitation of the technique would be the requirement for it to generalise, i.e. to operate effectively for a range of textures. Our assessment of the algorithm proceeds in two stages. In this section we ignore the question of generality and test the *form* of the filter—each texture is processed by a filter designed specially for that surface. In the next section the impact on performance of the general filter is assessed. This experiment represents a more realistic test of the algorithm. By resolving our assessment into two distinct stages we believe we will gain a better understanding of the technique's performance.

We begin by estimating the model parameters for each texture in the test set. This is done by splitting the power spectrum of each texture into fourteen radial frequency bands.The polar distribution of signal magnitude for each band is measured and a curve of the form $m\cos(\theta-\tau)+b$ is then fitted to the polar plot using least squares. The m and b parameters plotted against frequency in *Figure 7.3.3*. For both parameters the family of parameter curves can immediately be split into two groups which correspond to whether the surface is fractal (surfaces 1&2) or of the Mulvanney type (surfaces 3&4). The fractal textures exhibit a gradual decline in the value of the *m*-parameter with frequency, whereas for the Mulvanney surfaces the parameter actually increases before saturating. In the case of the *b*-parameter the Mulvanney surfaces are largely independent of frequency while the fractals show a significant drop with frequency. We therefore conclude that the form of the filter is a function of the surface type.

In our first application of the filters we postpone the issue of optimality and treat each texture independently. The F2 model is fitted to and applied to each texture. This involves fitting linear functions of frequency to both the parameter curves. We then examine the output of the 0 and 90° features of the f64 filter set, which is concentrated in the model's linear region ($\omega<0.25\omega_s$). In all the compensated cases the variation of feature output with tilt angle is much flatter, i.e. more stable than the uncompensated outputs (*Figure 7.3.4* and *Figure 7.3.5)*. However, we note the decrease in the effectiveness of the filters with the rougher surfaces. Even with F2 filters optimised to a particular texture the effect has not been eliminated.

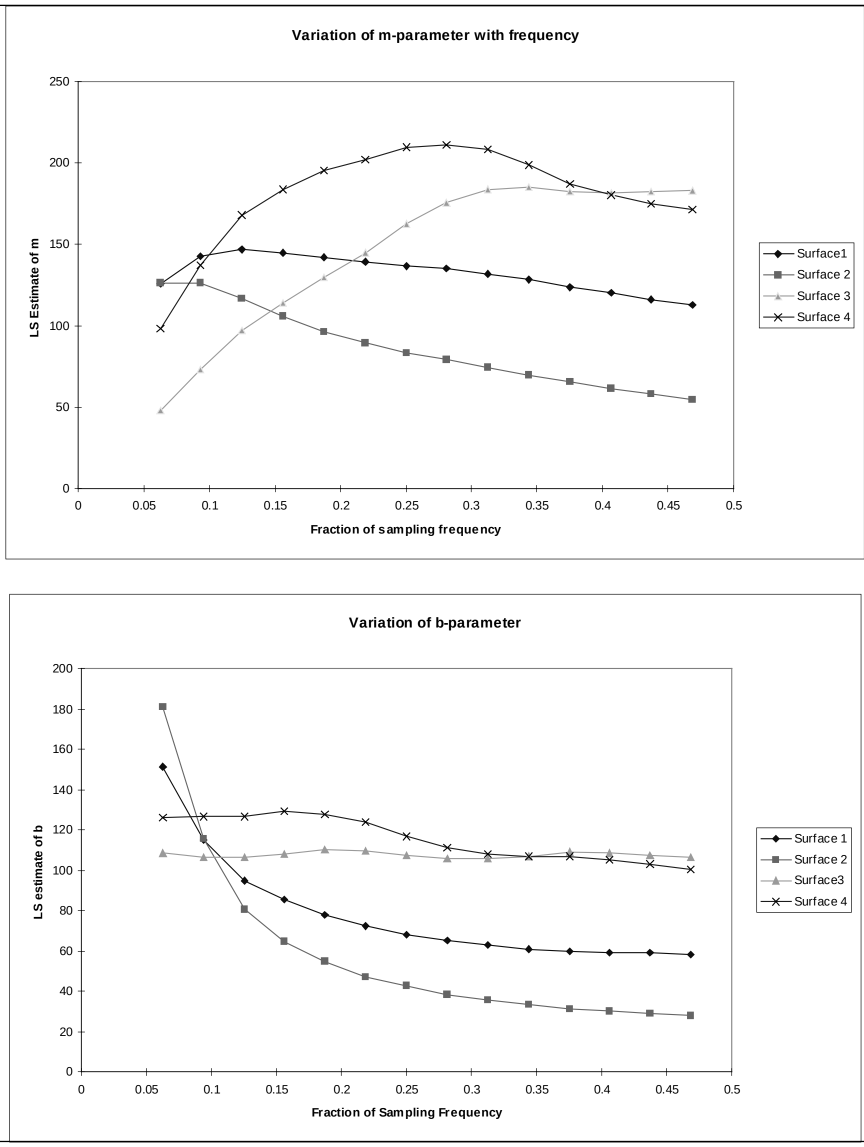

Figure 7.3.3 Frequency dependency of filter parameters for test textures.

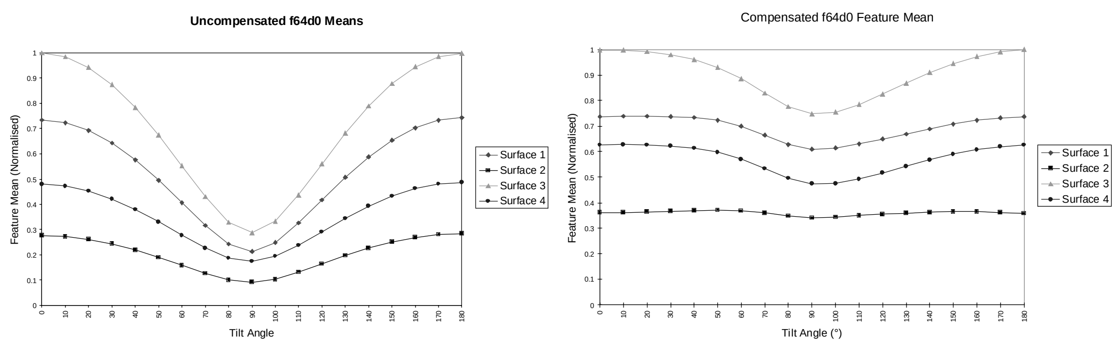

Figure 7.3.4 Uncompensated and compensated F64d0 feature means.

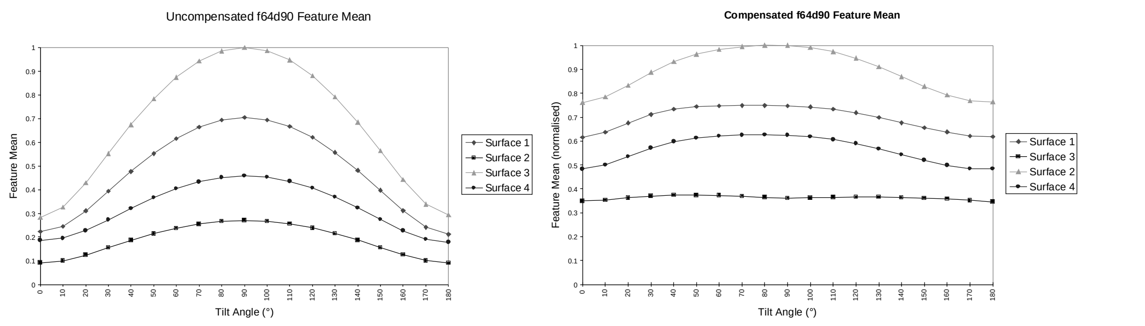

Figure 7.3.5 Uncompensated and compensated F64d90 feature means.

7.3.3 A General Filter

As stated earlier, for segmentation purposes we must adopt filter parameters which are a compromise for the textures in the test set. The compromise parameters are are estimated by averaging the *m* and *b* parameters associated with each texture and are plotted against frequency in *Figure 7.3.6,* linear functions of frequency are then fitted to both of these parameter curves. Application of the compromise filters shows a marked decrease in the stabilising properties of the filter (*Figure 7.3.7)*. If we classify on the basis of the two compensated filters we find that misclassification rates quickly rise to an unacceptable level (*Figure 7.3.8*).

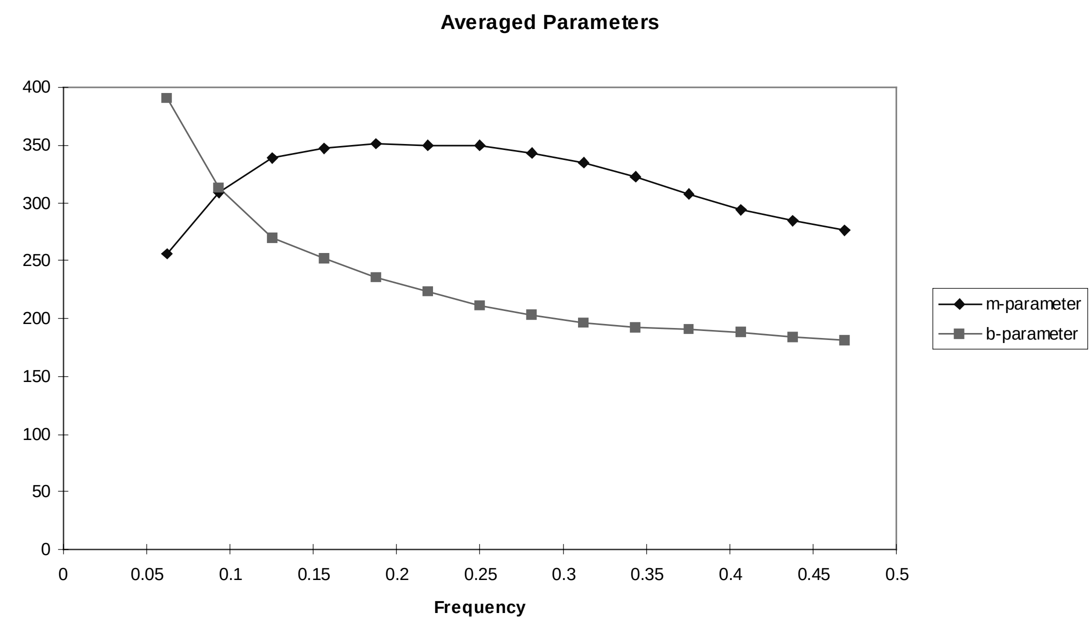

Figure 7.3.6 'General' filter parameters.

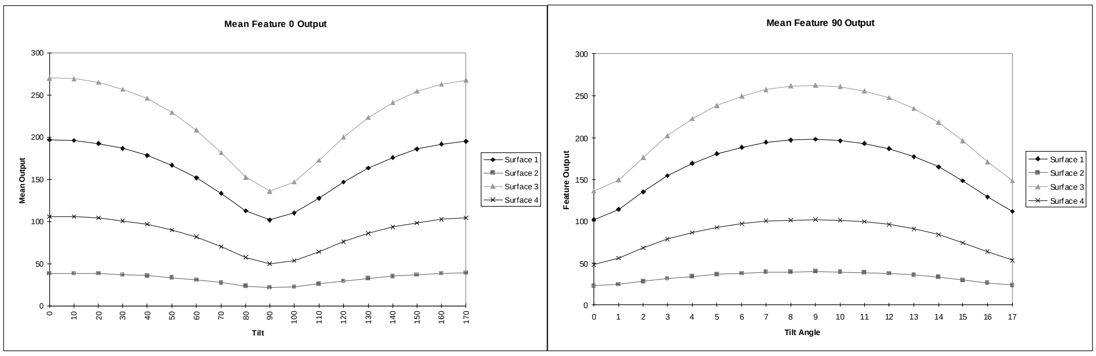

Figure 7.3.7 Feature means compensated using 'general' filter.

The filters do seem to work effectively on certain textures, specifically those with low slope angles and which are fractal within the corrected frequency range. In combination with the isotropy condition we believe the range of textures to which the technique is applicable is limited. We therefore conclude that this approach does not form an effective general approach to the problem of tilt induced failure.

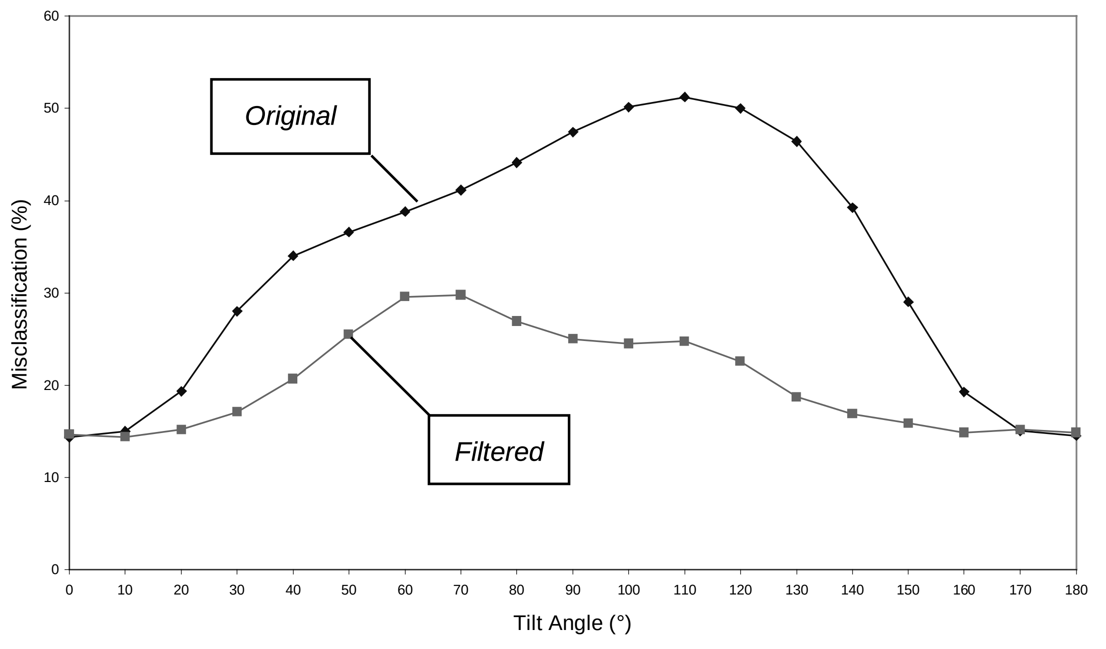

Figure 7.3.8 Misclassification rate of original and compensated montage.

7.4 *Single Image Shape From Shading Techniques*

7.4.1 Motivation

The goal of this thesis is to develop a scheme which can classify objects on the basis of their surface texture. There are a wide variety of texture analysis techniques which may be applied to the classification of a textured image. However, classification of surfaces on the basis of the appearance of textures is only valid if appearance is invariant under all conditions likely to be encountered. Chantler has shown that, for a large class of textures, changes in lighting orientation can radically alter the appearance of the texture [Chantler94]. This would suggest that where illumination direction, *relative to the texture*, cannot be strictly controlled, classification based purely on the appearance of a texture may not be an appropriate approach.

Classification of rough surfaces should ideally be carried out on the basis of the texture's surface, rather than its image structure, i.e. either on $s(x,y)$ or $\mathbf{S}(x,y)$ instead of $i(x,y)$. Several approaches exist for the recovery of surface topography, however shape from shading (SFS) is the most suited to our requirements since it does not require hardware additional to that already used for the classification task. Use of a single image SFS technique is particularly attractive since it would operate on the same data set as a naive classifier. The classifer would need only relatively minor modifications, applying the same texture analysis techniques to the surface representation rather than the image.

Shape from shading techniques have been used in computer vision for a quarter of a century, for most of this time they have been restricted to smooth surfaces. More recently, [Horn90] has applied the technique to complex wrinkled surfaces, while Pentland has applied his own novel technique to fractal surfaces [Pentland90]. This section will briefly describe the main approaches to shape from shading before examining the difficulties peculiar to their application to textures; finally the various techniques will be assessed in light of these difficulties.

Shape from shading techniques tend to capture high frequency surface variations, though they appear less adept at recovering low frequencies [Frankot88]. This seems to be true for human image interpretation [Knill90a]. Pentland [Pentland88] suggested the combination of low frequency data from a binocular stereo system and high frequency information from SFS techniques in the frequency domain. This was recently successfully implemented by Cryer et al. [Cryer95] by filtering stereo and shading derived depth maps with low pass and high pass filters respectively. Since we are concerned with textures, we are principally interested in the higher frequencies; shape from shading therefore seems to be a promising approach.

7.4.2 Shape From Shading

Introduction

Recovery of shape from shading is an ill-posed problem; a particular intensity value may be caused by any one of an infinite number of surface orientations. The intensity/orientation relationship for a given surface type is described by the reflectance map. This has the form shown in *Figure 7.4.1* where each contour corresponds to a particular image intensity. Therefore a surface facet with a particular intensity may have any orientation *p,q* which lies on the appropriate contour. There are some intensities which do correspond to a single orientation, e.g. maxima, these are known as singular points. However most intensities are not in this category and cannot be mapped uniquely to a single orientation. This ambiguity is the central problem of shape from shading, and the various SFS algorithms can be categorised by the approach they adopt to solve this problem.

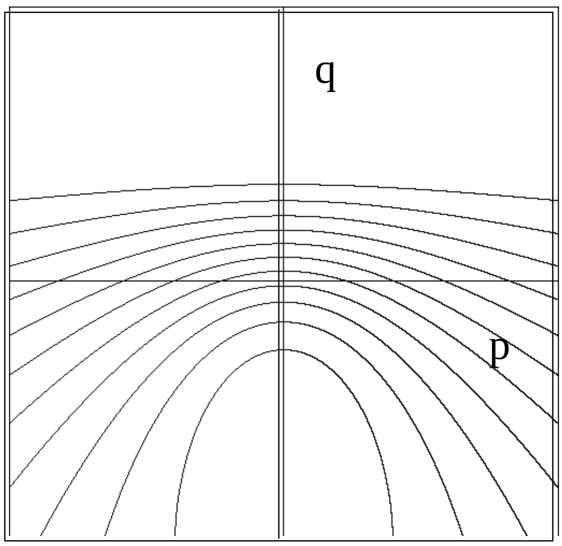

Figure 7.4.1 General form of the reflectance map

Classical Methods

The first attempt to solve the shape from shading problem was proposed by Horn [Horn70]. This treated the problem as that of solving a first order non-linear partial differential equation. Proceeding from a singular point the equation was solved to give characteristic curves of known orientation which were then grown to give the orientations of the entire surface. This technique has several difficulties: it has not been amenable to computer implementation, it is sensitive to measurement noise, and the areas grown from characteristic strips do not always merge well. This technique has largely been superceded by iterative schemes.

Iterative Techniques

Many iterative schemes have been proposed since [Strat79], most iterate on two criteria: the closeness of the simulated image of the recovered surface to the original image, and the smoothness of the resulting surface. Several algorithms also include integrabilty as a criterion—equation 7.4.2a is cited in [Zheng91] as a typical cost function:

$$\iint \left[i(x,y)-o(p,q)\right] + \lambda_s(p_x^2+p_y^2+q_x^2+q_y^2)+\mu_s\left[(z_x-p)^2+(z_y-q)^2\right]dxdy \quad (7.4.2a)$$

Closeness of intensity Smoothness Integrability

where λ_s, μ_s are constants,

$o(p,q)$ is the reflectance map

p_x, q_x, p_y, q_y, are the second derivatives

z_x and z_y are the derivatives of the estimated surface reconstruction.

The smoothness term restricts the applicability of the algorithm to smooth surfaces, and even for smooth surfaces may prevent convergence to the optimum. Recently however, there has been a more critical approach to the use of the smoothness criterion. Horn presents several refinements to the system, these include representation of both height and gradient to enforce integrability, a local linearisation of the reflectance map around the current gradient estimate and the ability to suppress the smoothing term as the optimum is approached [Horn90]. Using these techniques he is able to recover complex wrinkled surfaces.

Zheng and Chellapa have pointed out that most smoothness terms take no account of abrupt changes in the original image, and among other results, he presents a modified smoothing term [Zheng91]:

$$\left[R_p(p,q)p_x + R_q(p,q)q_x - I_x(x,y)\right]^2 + \left[R_p(p,q)p_y + R_q(p,q)q_y - I_y(x,y)\right]^2$$

Although Zheng conducted his experiments on locally smooth surfaces, in several images it is possible to observe discontinuities, albedo was also recovered.

A Frequency-Based Approach

In a highly original paper [Pentland90] operates in the frequency domain to recover complex surfaces including a synthetic fractal surface. Pentland uses a linearised form of the Lambertian equation as an invertable transform. This can be applied to the frequency domain representation of the original image and the resulting image can be returned to the spatial domain to yield the surface. The inverse transform is shown in Eq. 7.4.2b. Pentland has developed a modified version of this, incorporating a Wiener filter to suppress noise and non-linearities in the image, Eq. 7.4.2c.

$$H(\omega,\theta) = \frac{e^{-i\pi/2}}{2\pi\omega\left[k_1\cos\theta + k_2\sin\theta\right]} \qquad (7.4.2b)$$

where $k_1 = \cos\tau \sin\sigma$

and $k_2 = \sin\tau \sin\sigma$

$$H(\omega,\theta) = \frac{e^{-i\pi/2}}{2\pi k_o\omega\left[sd + k_1\cos\theta + k_2\sin\theta\right]} \qquad (7.4.2c)$$

where s= Signum[cos(τ-θ)]

and d is in the range 0.5 to 0.7

Since the Lambertian equation has been linearised, surface components perpendicular to the illuminant direction are not illuminated. The Fourier components of these patches must either be set to a default value, or estimated from other sources such as singular points. Pentland reports that using default values produces good approximations to complex and irregular surfaces, though it is less effective when dealing with regular geometric shapes. In a later paper [Pentland91] concerned with photometric effects in optical flow, Pentland uses a sequence of three images to first linearise the images before recovering both albedo and shape.

A Probabilistic System

Knill and Kersten [Knill90b] also use a linear approximation to the reflectance map as the basis for their Bayesian scheme. Rather than tackle the problem of under-determination by deterministic means, Knill seeks to use *a priori* knowledge of the surface type to estimate the most likely surface for a given image. Using 800 synthetic, illuminated, fractal surfaces as training data, Knill used the Widrow-Hoff algorithm to calculate the coefficients for two, 2 dimensional, FIR filters. These filters were used to model the mapping between the surface normals and the intensities of the corresponding pixel and those of its neighbours. Using the assumption of surface isotropy, variation in tilt angle is modelled by simple rotation of the masks.

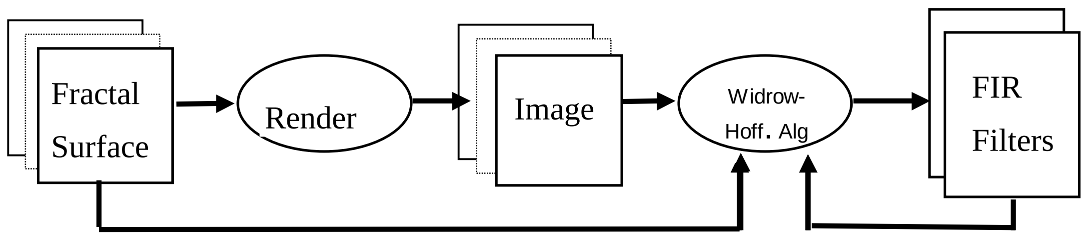

Figure 7.4.2 Deriving surface recovery filters.

The difficulty with the application of this scheme to the tilt-invariant problem lies in the requirement for *a priori* knowledge of the surface. It therefore follows that identification of the surface type is a prerequisite for the application of the optimum filter for surface recovery. Since, for our purposes, surface recovery is a means towards the end of identification this is clearly problematic, though if surfaces are sufficiently similar, it may be possible to apply a sub-optimal filter to recover the surfaces to a level of accuracy which will allow reliable classification.

7.4.3 Summary

Until recently, SFS techniques have been applied exclusively to predominantly smooth surfaces, and their application to textures raises several issues. If the texture surfaces are assumed to be fractal, then due to the self-similarity property, any smoothness in the image will be due to camera effects. Iterative techniques, unfortunately, use smoothness as a cost function. Horn's partial suspension of the criteria, and Zheng's rationalisation are both only partial solutions, and it seems unlikely that they will be effective in dealing with textures. Knill’s and Pentland's method make no smoothness assumption and will therefore be unaffected.

Knill’s and Pentland’s techniques represent the only techniques which we have been able to identify as being suitable for this problem. Although these schemes are both based on linear filtering, they do, however, differ in their derivation: Pentland’s scheme is deterministic, while Knill’s is probabilistic. Knill's technique is unsuitable for classification by definition: in order to employ *a priori* knowledge, the texture type must already be known.

In fact, closer examination of Pentland’s technique shows it to be almost identical to the independently developed Chantler’s filters. Although developed with different aims in mind, both techniques are derived from Kube and Pentland's linear model of the imaging process. The differences in the techniques are due to two factors: the different aims of the techniques and their treament of noise. In his F1 filter Chantler assumes noise to be white, though in the F2 filter he only assumes it to be isotropic and adopts an empirical approach to its radial frequency characteristics. Pentland assumes the noise spectrum is proportional to the image spectrum and develops his filter accordingly. The filters also differ in the purpose; Chantler only seeks to remove the directional effects of illumination and implicitly recovers the magnitude of the surface derivatives. Pentland aims to recover the surface height and therefore includes an $i\omega$ term to perform the integration of surface derivatives in the frequency domain. For our purposes these techniques are effectively the same, and will suffer from the same difficulties. We believe this equivalence to be quite revealing: Chantler's scheme is recovering a physically meaningful quantity— the magnitude of the surface derivative.

7.5 A Model-Based Approach Using Photometric Stereo

7.5.1 Model Based Classification

The model based approach is designed to anticipate the feature space distributions by modelling the underlying physical and analytical processes of imaging and feature extraction (*Figure 7.5.1*). This technique forms a spatial model of the training surfaces in the primary training stage. The classification process proper, begins with secondary training, when the recovered surfaces are synthetically rendered under the experimental conditions, and the resulting images form the basis of training. If the model’s components, the reflectance function and the surface description, are sufficiently accurate we should be able to obtain classification rates approaching those of the 'best case' classification, i.e. based on training on images obtained from surfaces illuminated at that tilt angle.

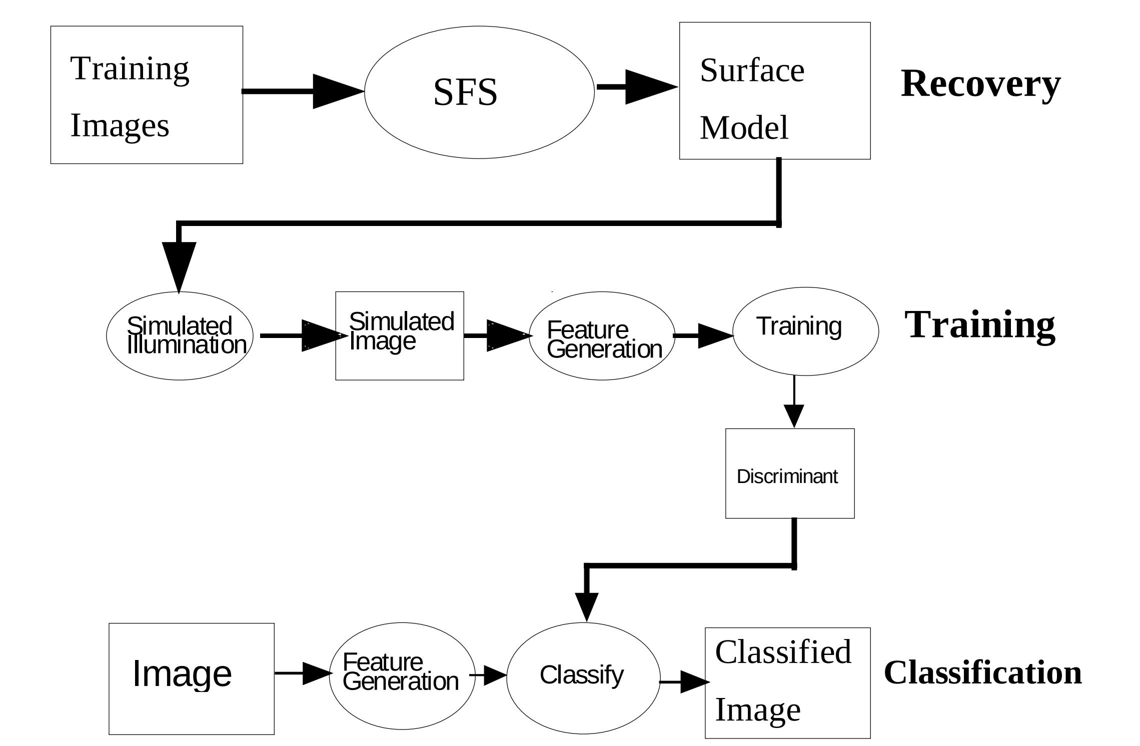

Figure 7.5.1 Simulation Based Classification

While we have an experimentally verified reflectance model for our textures (Chapter 3), we must still obtain the second component of the model: a description of the surface. To do this, a method of recovery must be adopted. As we discussed earlier, several cues to surface recovery have been investigated: focus [Noguchi94], binocular stereo [Papadimitriou95], and laser based approaches [Gross95], have been used. Let us assume that we will be able to invest more effort and exert more control in the recovery stage than in the classification stages. Ideally, we seek a technique which requires no additional hardware beyond that required for the classification.

The technique of photometric stereo allows us to form a surface description from several images of the same surface imaged under various illumination directions. It therefore seems ideally suited to our purposes since our problem is itself caused by variations in illuminant direction. In fact, surface representations acquired with photometric stereo has been used for modelling purposes by other authors. Russell

[Russell91] used photometric techniques to acquire depth maps which could then be synthetically illuminated to simulate aerial images.

7.5.2 Photometric Techniques

One approach to the SFS problem of under-determination is the use of photometric techniques [Woodham79]. These involve the use of several images of the same scene though under different illumination conditions. Each illumination condition will have its own unique reflectance map, and a given point's intensity will vary accordingly. Therefore each image will define a unique set of possible orientations for each point. If three or more images are used then the intersection of these solution sets will contain only one orientation; it is also possible to recover the albedo of the facet.

Consider a Lambertian surface illuminated from a given illumination direction, this defines a reflectance map *o(p,q), Figure 7.5.2*. If we are given a facet's intensity under these conditions, we may conclude only that its surface derivatives lie on a particular contour on the *p*-*q*-plane. This is essentially the fundamental problem of shape from shading; single image techniques use constraints in the spatial domain to resolve this ambiguity. Photometric techniques on the other hand use several images, imaged under different illumination conditions, with their own specific reflectance map. We therefore have a set of contours. The facet's derivatives are invariant and will lie at the intersection of these contours. Since two contours may overlap at more than one point we require three images to resolve ambiguities in all cases.

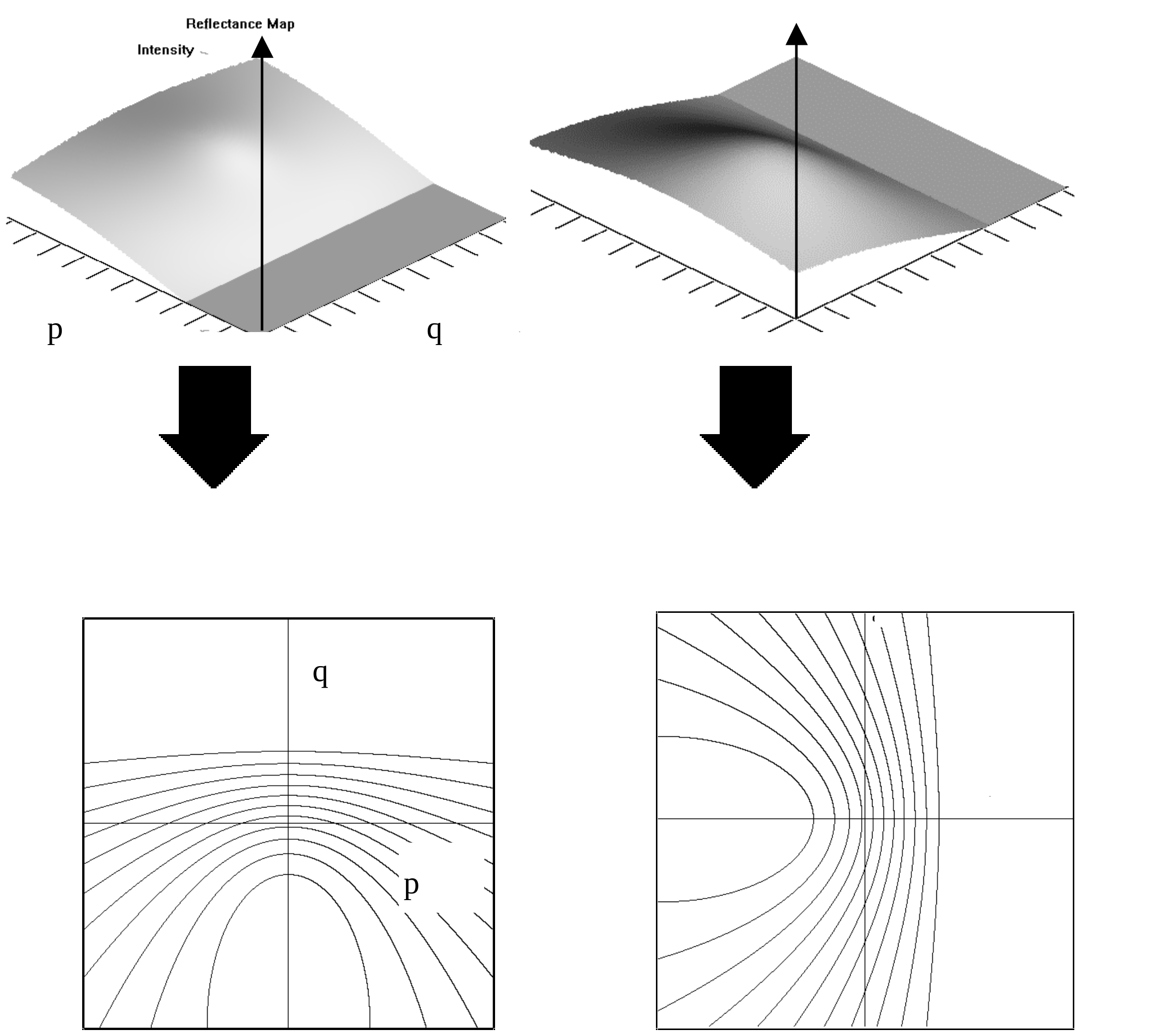

Figure 7.5.2 Reflectance Maps o(p,q) at τ 0° and 90°

More rigorously, consider Lambertian reflectance, where **L**,**S** and *I* represent the illuminant vector, normal vector and facet intensity respectively.

I=**L.S** where $$\mathbf{L} = [l_1, l_2, l_3]$$ $$\mathbf{S} = [p, q, 1]$$

Now, consider the same facet illuminated three times with different illuminant vectors: define: $\mathbf{I_{ph}} = [i_1, i_2, i_3]$ and the combined illuminant vector $L_{ph} = \begin{bmatrix} l_{11} & l_{12} & l_{13} \\ l_{21} & l_{22} & l_{23} \\ l_{31} & l_{32} & l_{33} \end{bmatrix}$

Reiterating

$$I_{ph}=\mathbf{S}.\mathbf{L_{ph}} \qquad \text{and} \qquad \mathbf{I}_{ph}.\mathbf{L}_{ph}{}^{-1} = \mathbf{S}$$

While this may be solved numerically, most implementations use three dimensional lookup tables.

In this section we have proposed a simulation based scheme which is designed to counteract the effect of tilt on classification by predicting the location of feature space distributions for given tilt conditions. This is achieved by using a surface and a reflectance model to generate training data which is appropriate to classification under the specified illumination conditions.

The surface model is an important component in the scheme. We have identified, and given a brief description of, a technique which is capable of recovering the required model, with relatively little overhead in terms of additional hardware and training.

7.6 Conclusions

In this chapter we considered three techniques proposed by Chantler [Chantler94] for the reduction of tilt induced misclassification, as well as surveying the field of shape from shading and proposing a novel simulation based technique.

Chantler's first technique attempted to make the classifier robust by training the classifier over the range of illumination conditions which occur during the classification sessions. Examination of the feature means for two test textures showed that it is not safe to employ a single threshold to discriminate between textures throughout the tilt range. This result also showed that, in practice, the tilt angle must be known before the classification may be undertaken.

Chantler's second proposal advocated the use of a family of discriminants indexed by tilt angle. Application of this technique to our test montages showed that, while the technique is effective at reducing tilt degradation at the training angles, the misclassification rate quickly increases as the illuminant tilt moves away from these angles. From the performance of the classifier on our montages, we believe that a new discriminant must be designed at intervals not exceeding 20° of tilt.

Chantler also defined a system of filters which are based on inverting the directional effects modelled by Kube and Pentland, [Kube88]. We found application of this scheme to be limited for two reasons. The first is the requirement that test surfaces are isotropic; this condition is associated with the implementation of the filter estimation, and it is possible to suggest an alternative scheme using more than one estimation image to generalise the technique to directional surfaces. A more serious drawback is that of generality; the characteristics of a filter are specific to a particular surface and any general filter must be sub-optimal. In our experiments we found that, even with the isotropy restriction, the sub-optimal filter is unable to stabilise the features to a satisfactory degree. We do not pursue this approach further.

The field of single image shape from shading was reviewed. Mainstream SFS algorithms use a smoothness constraint and are therefore unsuitable for texture classification. Two techniques have been applied to fractal surfaces, however, implicit in both is the requirement for *a priori* information as to the nature of the surface. This, by definition, rules out these techniques from further investigation.

Finally a model based technique was proposed. This uses an estimate of the surface derivative field obtained using photometric stereo to predict the observed texture under specified illumination conditions. This prediction is then used to train the classifier for those illumination conditions. The next chapter will describe the evaluation of this technique.